Editors' Suggestion

Plastic Deformation in a Quantum Solid: Dislocation Avalanches and Creep in Helium

Zhi Gang Cheng[1,2,*] and John Beamish[2,†]
[1]Beijing National Laboratory for Condensed Matter Physics, Institute of Physics, Chinese Academy of Sciences, Beijing 100190, People's Republic of China
[2]Department of Physics, University of Alberta, Edmonton, Alberta, Canada T6G 2E1

(Received 6 April 2018; published 30 July 2018)

Conventional solids deform elastically for small stresses—reversibly with a linear, rate-independent relationship between stress and strain. Beyond the yield point, plastic deformation begins—irreversible, nonlinear, and time dependent. Plasticity involves the motion and multiplication of dislocations, and here we report observations of such "metallurgical" phenomena in hcp ^{4}He, a solid whose defect behavior is dominated by quantum effects. Below 0.4 K, there is a strain threshold for elastic deformation above which sudden stress drops and acoustic emissions appear, the signatures of dislocation avalanches. The dimensions of these slip events range from millimeters to microns. At higher temperatures, the avalanches are replaced by continuous creep involving dislocations, and we observe steady flow at stresses as low as 400 Pa.

DOI: 10.1103/PhysRevLett.121.055301

The elasticity, ductility, and brittleness of metals are associated with dislocations and impurities, whose motions are usually thermally activated. At a microscopic level, plastic deformation is a complex phenomenon, with pinning, multiplication, and entanglement of dislocations leading to yield drops and work hardening. At high temperatures and low strain rates, thermally activated creep allows solids to deform smoothly, at rates that increase with the temperature and applied stress. At lower temperatures, flow can occur intermittently, via sudden dislocation avalanches. Experiments on ice [1–4], metals, and alloys [5–8] have shown that these avalanches can have a wide distribution in length and time. Avalanche events are initiated when the local stress is large enough for dislocations to overcome obstacles, allowing them to move and multiply. They end when the dislocations form an entangled network and are immobilized. The size and duration of an avalanche depend on the speed at which dislocations move. Even at very high stresses and strain rates, dislocation motion is usually strongly damped [9], with speeds limited by the drag due to scattering of thermal phonons [10] and, in metals, of electrons [11].

As a model system to study defects and their impact on mechanical properties, solid helium has unique advantages over conventional solids. Measurements can be made over the full temperature range from melting (T_m) to near zero ($0.01T_m$), where thermal effects, including dislocation damping, are negligible. Impurity effects can be eliminated, since ^{4}He crystals can be grown completely free of all but isotopic (^{3}He) impurities, which can be reduced to concentrations as low as 10^{-12}. Also, helium crystals are highly quantum mechanical, and their defects are extraordinarily mobile even near absolute zero, allowing crystals to respond in surprising ways.

Supersolidity, the coexistence of crystalline and superfluid order, is the most dramatic quantum phenomenon proposed for ^{4}He crystals. Claims of its discovery in a 2004 experiment [12,13] led to an explosion of experimental and theoretical works, but it is now clear that the torsional oscillator period shifts reflected unexpected elastic effects due to defects [14–16] instead of mass decoupling. At low temperatures, dislocations in hcp ^{4}He crystals glide freely in the basal plane, with no Peierls barrier ($\sigma_P < 10^{-3}$ Pa) [15]. The only impurities, ^{3}He atoms, are not effective pinning centers, since they propagate freely as "impuritons" at low speeds and break away from dislocations at stresses above 1 Pa [17]. At temperatures below 0.4 K, thermal damping is negligible, and the dislocations' extraordinary mobility can reduce the shear modulus by more than 80%, an effect referred to as giant plasticity [15].

Early plastic deformation experiments on ^{4}He [18–21] involved modified versions of conventional stress-strain measurements, made at high temperatures where thermal processes play an important role. It is clear that at high temperatures hcp ^{4}He crystals flow via defect creep, but subsequent measurements [22–25] showed that thermally activated defect motion freezes out, and no plastic flow was seen below 0.5 K. The picture that emerges is one in which, despite helium's extraordinary softness (shear modulus and yield stress are $\sim 10^4$ times smaller than for typical metals [26]), high-temperature plastic deformation involves mechanisms similar to conventional crystals. Until now, however, there have been no direct observations of plastic flow at low temperatures where quantum effects dominate.

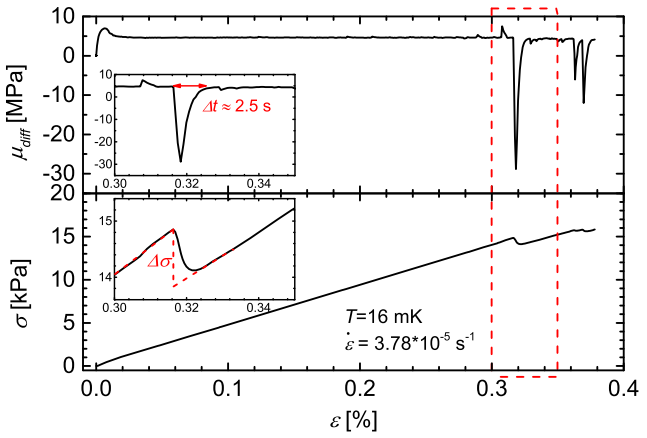

FIG. 1. $\mu_{\rm diff}$ (top) and σ (bottom) while ramping ε at 16 mK with $\dot{\varepsilon} = 3.78 \times 10^{-5}$ s^{-1}. Insets are expanded views of the dashed red box. The stress release $\Delta\sigma$ should occur in a timescale much shorter than the apparent width of the event as indicated by the dashed lines (see the text).

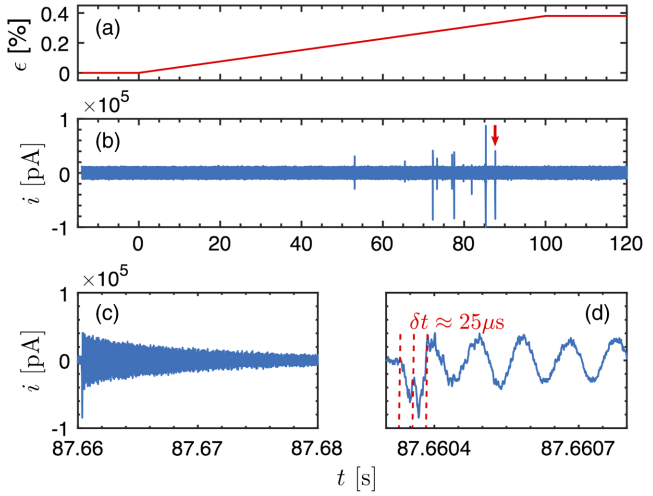

FIG. 2. Fast data with a linear strain ramp shown in (a). The spike labeled by an arrow in (b) is shown on expanded timescales in (c) and (d). The initial event (width ~25 μs) is followed by decaying oscillations at a frequency of ~10.5 kHz.

In this Letter, we describe shear deformation experiments on hcp ^{4}He at temperatures as low as 16 mK. Below 0.4 K, the response was elastic up to strains of about 0.2%. At higher strains, we observed sudden slip events accompanied by acoustic emissions (AEs), which we identify as dislocation avalanches. Above 0.5 K, these avalanches disappeared and deformation occurred via thermal creep but with flow stresses orders of magnitude smaller than in conventional crystals.

All samples reported in this Letter were prepared with ^{4}He gas with a ^{3}He impurity concentration of 120 ppb. The measurements were performed in a similar setup to shear modulus measurements in the elastic region [14,15], with the driving piezoelectric transducer (lead zirconate titanate–PZT) replaced by a stack PZT actuator. Details can be found in Supplemental Material [27]. The differential shear modulus $\mu_{\rm diff} = d\sigma(t)/d\varepsilon(t)$ and shear stress σ are plotted versus strain ε in Fig. 1 for an hcp ^{4}He sample at $T = 16$ mK. The strain was ramped with a rate $\dot{\varepsilon} = 3.8 \times 10^{-5}$ s^{-1}, reaching a maximum strain $\varepsilon_{\rm max} = 0.38\%$. For $\varepsilon < 0.2\%$, $\sigma \propto \varepsilon$, giving $\mu_{\rm diff} \simeq 50$ bar. For $\varepsilon > 0.2\%$, we observed abrupt changes visible as spikes in $\mu_{\rm diff}$, most of which were negative, i.e., releases of stress $\Delta\sigma$. These appeared randomly and reflect plastic slips within the solid. Sliding, e.g., due to a liquid layer between the solid helium and the transducers, would also reduce the stress. However, it would not plastically deform the bulk helium and create large numbers of dislocations that change the solid elastic properties [14,15]. We measured the shear modulus with $\varepsilon < 10^{-6}$ before and after plastic deformation and found a significant stiffening caused by the deformation [27]. Thus, at least some of the slips must occur within the solid. Also, the slips were less frequent during subsequent deformations, as expected when work hardening increases the dislocation density. We repeated the deformation at temperatures up to 0.5 K. Below 0.1 K, the $\mu_{\rm diff}$ spikes were distributed randomly above $\varepsilon_s = 0.2\%$, showing no obvious temperature dependence. Above 0.2 K, the spikes were smaller and began at larger strains ε_s. At 0.5 K, we saw no spikes up to 0.38%, only thermal creep.

The largest slip in Fig. 1 gives to a stress drop $\Delta\sigma \simeq 6\%$. Since the measured stress is averaged over the entire transducer surface of 1 cm^2, $\Delta\sigma$ could be due either to a complete relaxation over 6 mm^2 or to a partial relaxation over a larger area. The apparent duration of $\Delta t \simeq 2.5$ s reflects the rise-fall time (1 s) of our lowest noise preamplifier; the real slip time is much shorter. To resolve the slip dynamics, we repeated the measurement after thorough annealing, using a 100 kHz preamplifier (4 μs rise-fall time). Its gain was ~10^6 times lower, but slips are still visible in Fig. 2(b). As shown on expanded timescales [Figs. 2(c) and 2(d)], a typical event begins with an irregular stress drop followed by a decaying oscillation. The initial drop occurred over $\delta t \simeq 25$ μs and triggered an acoustic resonance of the helium in the entire cell [27]. The resonance frequency (10.5 kHz) and quality factor ($Q = 300$–500) are similar to those of acoustic resonances previously seen in solid helium [14]. We also used a voltage preamplifier and a digital oscilloscope to capture even faster events. Figure 3 shows a typical event with a duration of about 0.6 μs and a broad frequency spectrum around 20 MHz. This is much higher than any acoustic resonance in the helium or the transducers (e.g., helium in the 170 μm gap would resonate at around 600 kHz; the sensing transducer has a fundamental resonance of 1.7 MHz [29]). This signal must originate from a much smaller region of the helium.

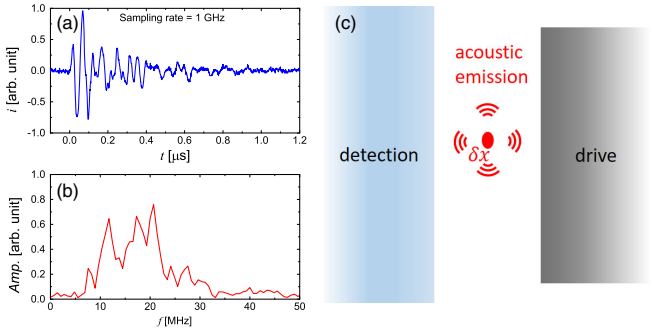

FIG. 3. (a) AE event and (b) its Fourier transform. (c) Schematic of AE from a slip region with size δx much smaller than the gap between transducers.

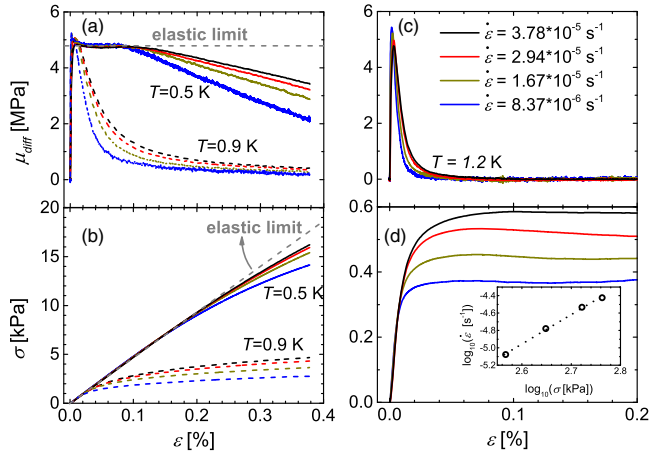

FIG. 4. $\mu_{\rm diff}$ (a),(c) and σ (b),(d) versus ε for different strain rates $\dot{\varepsilon}$ at $T = 0.5$, 0.9, and 1.2 K. Color codes for different $\dot{\varepsilon}$ are shown in (c) and apply to all panels. The inset in (d) is a log-log plot of $\dot{\varepsilon}$ versus σ at $T = 1.2$ K and $\varepsilon = 0.1\%$. A power-law fit $\dot{\varepsilon} \propto \sigma^n$ is plotted with a dashed line, giving an exponent $n \simeq 3.38$.

Intermittent plastic events have been seen in many conventional solids. They are associated with dislocation avalanches. They are usually detected indirectly from their AEs in bulk materials. The sudden stress releases associated with avalanches have been directly observed in very small samples, including Ni microcrystals [30,31] and Cu nanopillars [32]. Avalanches begin when local stresses break dislocations away from pinning sites, so they can move and multiply. Dislocation motion is driven by the force exerted by shear stress $F_{\rm drive} = b\sigma l$, where b is the dislocation's Burgers vector and l its length. The damping force $F_{\rm damp} = Bvl$, where v is the dislocation speed and B the damping coefficient, limits their speed to $v_f = b\sigma/B$. The damping is due to scattering of thermal phonons and (in metals) electrons. In copper and aluminum, e.g., damping limits $v_f \simeq 10$ m/s for MPa applied stresses [8,10]. Even at the extremely high strain rates ($\dot{\varepsilon} \sim 10^6$ s^{-1}) in shock experiments, typical dislocation speeds are much less than the sound speed [33]. The effective mass of dislocations is small, so they accelerate and reach their maximum speed in about a nanosecond, over a distance of a few nanometers [9]—avalanches in conventional solids occur in a regime where dislocation motion is strongly damped.

In contrast, dislocations in helium move freely at low temperatures. There is essentially no impurity pinning for large stresses, and the only damping is due to thermal phonons, giving $B \simeq 1.5 \times 10^{-8} T^3$ Pa s [17]. For ^{4}He near melting ($T_m = 1.55$ K), this limits dislocations to about 50 m/s for a shear stress of 10 kPa. However, at 16 mK the phonon damping force is negligible (< 0.04 Pa), even for dislocations moving at the speed of sound ($v_t \simeq 200$ m/s). In the absence of damping, a stress of 10 kPa will accelerate dislocations to the sound speed in about 2 ns over a distance of $\simeq$200 nm. We expect avalanches in helium to move at close to their theoretical maximum velocity, the speed of sound v_t, and stop only when they are immobilized by entanglements or grain boundaries. The submicrosecond AE events in Fig. 3 involve frequencies around 20 MHz, much faster than slip events in ice and metals with frequencies below 1 MHz and durations from tens of microseconds to milliseconds [3,34,35]. Even though solid helium has sound speeds an order of magnitude slower than conventional solids, its dislocation avalanches can be much faster.

The size of avalanches can be estimated from their timescales. For example, the large slip event shown in Fig. 2(d) has $\delta t \simeq 25$ μs, which limits the source of the initial stress drop to a region smaller than $v_t \delta t \simeq 5$ mm, consistent with the minimum slip area inferred from the 6% stress drop in Fig. 1. The small event in Fig. 3 is even faster, with a frequency spectrum centered around 20 MHz, and must originate in a much smaller region. An avalanche propagating at speed v_t in a region of size δx generates sound at frequencies around $f = v_t/2\delta x$, so this slip must occur in a region of size $\delta x \simeq 5$ μm. The dislocation density in polycrystalline solid ^{4}He has been estimated [36] as $\Lambda = 10^6$ cm^{-2}, giving an average separation between dislocations $d \sim 10$ μm. This suggests that events like that shown in Fig. 3 are due to the ballistic glide of a small number of undamped dislocations, perhaps only one, at velocities close to the speed of sound.

Figure 4 shows helium's flow response at temperatures above 0.5 K for constant strain rates in the range $\dot{\varepsilon} = 8.37 \times 10^{-6} - 3.78 \times 10^{-5}$ s^{-1}. At 0.5 K, helium stays on the elastic limit up to $\varepsilon \simeq 0.08\%$ and then begins to deform plastically, reducing σ and $\mu_{\rm diff}$ below the elastic limits as shown in Figs. 4(a) and 4(b). The shear modulus, $\mu_{\rm diff} \simeq 50$ bar and consistent with that at lower temperatures, is smaller than the intrinsic value for defect-free ^{4}He crystals ($C_{44} \simeq 124$ bar [26]). This is typical of the "soft" shear modulus in crystals containing mobile dislocations [15], since ^{3}He impurities are too weakly bound to pin dislocations at high strains. As the strain is increased further, slow plastic flow appears as creep and is associated with thermally activated motion of defects, e.g., vacancy

diffusion or dislocation glide and climb. At 0.9 K, plastic deformation began at smaller strains and was much faster, indicating its thermal origin. This is even clearer at 1.2 K, about 0.35 K below T_m, as shown in Figs. 4(c) and 4(d). The creep began immediately when strain was applied, and for $\varepsilon > 0.1\%$ the solid deformed at a constant flow stress of about 0.4 kPa, 4 orders of magnitude smaller than helium's elastic shear modulus. This is quite different from the behavior at the lowest temperature, where, as long as the strain does not exceed the elastic limit where avalanches begin, strain cycles are reversible with nearly linear stress-strain curves. The small hysteresis at low temperatures [27] may just be an artifact of electrical cross talk between the driving stack and the detecting transducer.

As expected, the flow stress increases with an increasing strain rate. The power-law relation between σ and $\dot{\varepsilon}$ provides information about the creep mechanism. For diffusional creep of vacancies (Nabarro-Herring creep) [37], the relation is linear: $\dot{\varepsilon} \propto \sigma$. This mechanism dominates for high temperatures and small grain sizes, e.g., solid ^{4}He confined in the nanoscale pores of Vycor glass [38]. At lower temperatures or for larger grains, creep involves dislocations as well as vacancies [39], and the power law $\dot{\varepsilon} \propto \sigma^n$ has exponent $n \geq 3$, consistent with our observation $n \simeq 3.4$ as shown in the inset in Fig. 4(d).

High-temperature creep has been seen in previous measurements [18,19,21] on hcp ^{4}He, but flow stresses were 1–2 orders of magnitude larger than in Fig. 4(d). This may reflect the larger strain rates used in those experiments (1–3 orders of magnitude faster than ours), the crystals' higher pressures (32 versus 26.4 bar), and the complex flow geometries (e.g., around a sphere moving through the helium) which involved multiple slip systems. Measurements on crystals in contact with liquid helium at 1.85 K showed lower flow stresses, and only an upper limit (< 5 kPa) could be determined [21]. Our better resolution allows us to measure much lower strain rates and flow stresses and to observe creep at much lower temperatures. There is no evidence of the yield drops reported in some of the early experiments [18,19], which may also have been due to the large strain rates of those measurements.

By combining direct measurements of the stress-strain relation and acoustic emissions in hcp ^{4}He, we have shown the importance of dislocations in the mechanical properties of this quantum solid. Recent quantum Monte Carlo simulations [40] concluded that a perfect helium crystal would retain its intrinsic shear strength up to strains of ~5%, but we found that the solid responds elastically at a low temperature only for strains up to ~0.2%. Sudden stress drops emerge at higher strains, accompanied by the AEs expected from dislocation avalanches. The dimension of the slip regions varies over at least 3 orders of magnitude, up to several millimeters. We recorded AE events with high frequencies (~20 MHz), which must originate in regions of only a few micrometers, comparable to the spacing between dislocations. In the absence of damping, hcp ^{4}He's mobile dislocations travel at speeds close to the sound speed, much faster than the damped dislocations in conventional solids. The low-temperature dislocation avalanches can increase the helium's elastic shear modulus, a form of work hardening. The shear modulus can be restored to its predeformation value by warming above 0.5 K. The ease with which the deformation effects can be annealed suggests that the avalanches do not produce the highly entangled dislocation networks that would be expected if multiple slip systems were involved. This is consistent with a picture of avalanches involving glide of the mobile basal plane dislocations.

The avalanches disappear above 0.5 K, replaced by smooth creep deformation involving thermally excited motion of dislocations. Previous experiments [28] have shown that thermal vacancies can anneal pressure gradients in hcp ^{4}He at temperatures above 0.5 K. Such vacancies allow dislocations to climb, enabling them to move past obstacles and newly created loops to disappear. A recent model [41,42] for plastic deformation in hcp ^{4}He includes the effects of multiplication and thermally activated motion of dislocations. The model predicts continuous deformation above a yield strain at a flow stress that increases with the strain rate. The authors applied their model as an alternate explanation of the "giant plasticity" seen in the shear modulus at temperatures below 0.3 K and at much lower strains ($\varepsilon \simeq 10^{-8}$) [15]. It does not predict the sudden avalanches we see at high strains in this temperature range, but with different parameters it could provide a framework to quantitatively understand the high-temperature behavior shown in Fig. 4.

The slips at low temperatures are quite different from the continuous motion seen in pressure-driven mass flow experiments on solid ^{4}He below 0.6 K [43–46]. This rules out plastic deformation as the mechanism of this mass transport, which has been interpreted in terms of superflow along a dislocation network. Superfluid dislocation cores would also allow dislocations to climb, even when there are no thermal vacancies. Such a superclimb [47,48] would provide a new deformation mechanism for quantum plasticity. However, despite the extraordinary mobility of dislocations, our measurements show that solid helium is "brittle" at low temperatures and deforms suddenly via dislocation avalanches. Our direct stress-strain relation measurements, the first to extend to such low temperatures, show that plastic deformation of this quantum crystal shares many features with metals and conventional solids but also has uniquely quantum behavior.

We thank Mark Freeman, John Davis, Joseph Losby, and Callum Doolin for help on fast data collection. This work was supported by a grant from Natural Sciences and Engineering Research Council Canada. Z. G. C. acknowledges the support from Ministry of Science and Technology (MOST) Grant No. 2018YFA0305604 and Hundreds Talent Program 2017-106, Chinese Academy of Sciences.

*zgcheng@iphy.ac.cn
†jbeamish@ualberta.ca

[1] J. Weiss and J.-R. Grasso, J. Phys. Chem. B **101**, 6113 (1997).
[2] M.-C. Miguel, A. Vespignani, S. Zapperi, J. Weiss, and J.-R. Grasso, Nature (London) **410**, 667 (2001).
[3] T. Richeton, J. Weiss, and F. Louchet, Acta Mater. **53**, 4463 (2005).
[4] T. Richeton, J. Weiss, and F. Louchet, Nat. Mater. **4**, 465 (2005).
[5] T. Richeton, P. Dobron, F. Chmelik, J. Weiss, and F. Louchet, Mater. Sci. Eng. A **424**, 190 (2006).
[6] M. A. Lebyodkin, I. V. Shashkov, T. A. Lebedkina, K. Mathis, P. Dobron, and F. Chmelik, Phys. Rev. E **88**, 042402 (2013).
[7] H. Hatano, J. Appl. Phys. **48**, 4397 (1977).
[8] W. Schaarwchter and H. Ebener, Acta Metall. Mater. **38**, 195 (1990).
[9] Z. Q. Wang, I. J. Beyerlein, and R. Lesar, Philos. Mag. **87**, 2263 (2007).
[10] J. A. Gorman, D. S. Wood, and T. Vreeland Jr., J. Appl. Phys. **40**, 833 (1969).
[11] J. Galligan, Scr. Metall. **18**, 653 (1984).
[12] E. Kim and M. H. W. Chan, Nature (London) **427**, 225 (2004).
[13] E. Kim and M. H. W. Chan, Science **305**, 1941 (2004).
[14] J. Day and J. R. Beamish, Nature (London) **450**, 853 (2007).
[15] A. Haziot, X. Rojas, A. D. Fefferman, J. R. Beamish, and S. Balibar, Phys. Rev. Lett. **110**, 035301 (2013).
[16] J. R. Beamish, A. D. Fefferman, A. Haziot, X. Rojas, and S. Balibar, Phys. Rev. B **85**, 180501 (2012).
[17] A. Haziot, A. D. Fefferman, F. Souris, J. R. Beamish, H. J. Maris, and S. Balibar, Phys. Rev. B **88**, 014106 (2013).
[18] H. Suzuki, J. Phys. Soc. Jpn. **35**, 1472 (1973).
[19] H. Suzuki, J. Phys. Soc. Jpn. **42**, 1865 (1977).
[20] V. L. Tsymbalenko, Sov. JETP Lett. **23**, 653 (1976).
[21] D. J. Sanders, H. Kwun, A. Hikata, and C. Elbaum, Phys. Rev. Lett. **39**, 815 (1977).
[22] J. Day, T. Herman, and J. Beamish, Phys. Rev. Lett. **95**, 035301 (2005).
[23] J. Day and J. Beamish, Phys. Rev. Lett. **96**, 105304 (2006).
[24] A. S. C. Rittner, W. Choi, E. J. Mueller, and J. D. Reppy, Phys. Rev. B **80**, 224516 (2009).
[25] A. Lisunov, V. Maidanov, N. Mikhin, A. Neoneta, V. Rubanskyi, S. Rubets, E. Rudavskii, and V. Zhuchkov, J. Low Temp. Phys. **175**, 113 (2014).
[26] J. Beamish, J. Low Temp. Phys. **168**, 194 (2012).
[27] See Supplemental Material at http://link.aps.org/supplemental/10.1103/PhysRevLett.121.055301, which includes Refs. [14,15,28], for measurement details, sample preparation and annealing, preamplifiers and data taking, shear modulus measurements and effects of low-temperature deformation, and acoustic resonance generated by slip events.
[28] A. Suhel and J. R. Beamish, Phys. Rev. B **84**, 094512 (2011).
[29] A. Tawfik, J. Am. Ceram. Soc. **68**, C-317 (1985).
[30] D. M. Dimiduk, C. Woodward, R. LeSar, and M. D. Uchic, Science **312**, 1188 (2006).
[31] S. Papanikolaou, D. M. Dimiduk, W. Choi, J. P. Sethna, M. D. Uchic, C. F. Woodward, and S. Zapperi, Nature (London) **490**, 517 (2012).
[32] X. Ni, S. Papanikolaou, G. Vajente, R. X. Adhikari, and J. R. Greer, Phys. Rev. Lett. **118**, 155501 (2017).
[33] M. A. Shehadeh, H. M. Zbib, and T. D. D. L. Rubia, Philos. Mag. **85**, 1667 (2005).
[34] M. A. Lebyodkin, T. A. Lebedkina, F. Chmelík, T. T. Lamark, Y. Estrin, C. Fressengeas, and J. Weiss, Phys. Rev. B **79**, 174114 (2009).
[35] I. Shashkov, M. Lebyodkin, and T. Lebedkina, Acta Mater. **60**, 6842 (2012).
[36] A. Haziot, A. D. Fefferman, J. R. Beamish, and S. Balibar, Phys. Rev. B **87**, 060509 (2013).
[37] C. Herring, J. Appl. Phys. **21**, 437 (1950).
[38] J. R. Beamish, N. Mulders, A. Hikata, and C. Elbaum, Phys. Rev. B **44**, 9314 (1991).
[39] J.-P. Poirier, *Creep of Crystals* (Cambridge Unviersity Press, Cambridge, England, 1985).
[40] E. J. Landinez Borda, W. Cai, and M. de Koning, Phys. Rev. Lett. **112**, 155303 (2014).
[41] C. Zhou, J.-j. Su, M. J. Graf, C. Reichhardt, A. V. Balatsky, and I. J. Beyerlein, Philos. Mag. Lett. **92**, 608 (2012).
[42] C. Zhou, J.-J. Su, M. J. Graf, C. Reichhardt, A. V. Balatsky, and I. J. Beyerlein, Phys. Rev. B **88**, 024513 (2013).
[43] Z. G. Cheng, J. Beamish, A. D. Fefferman, F. Souris, S. Balibar, and V. Dauvois, Phys. Rev. Lett. **114**, 165301 (2015).
[44] Z. G. Cheng and J. Beamish, Phys. Rev. Lett. **117**, 025301 (2016).
[45] Y. Vekhov, W. J. Mullin, and R. B. Hallock, Phys. Rev. Lett. **113**, 035302 (2014).
[46] J. Shin, D. Y. Kim, A. Haziot, and M. H. W. Chan, Phys. Rev. Lett. **118**, 235301 (2017).
[47] A. B. Kuklov, L. Pollet, N. V. Prokof'ev, and B. V. Svistunov, Phys. Rev. B **90**, 184508 (2014).
[48] A. B. Kuklov, Phys. Rev. B **92**, 134504 (2015).